Hemodynamic Profiles Before and After Surgery in Bicuspid Aortic Valve Disease—A Systematic Review of the Literature

Daniel G. W. Cave, Hannah Panayiotou and Malenka M. Bissell*

Department of Biomedical Imaging Science, Leeds Institute of Cardiovascular and Metabolic Medicine, University of Leeds, Leeds, United Kingdom

Bicuspid aortic valve (BAV) disease presents a unique management challenge both pre- and post-operatively. 4D flow MRI offers multiple tools for the assessment of the thoracic aorta in aortic valve disease. In particular, its assessment of flow patterns and wall shear stress have led to new understandings around the mechanisms of aneurysm development in BAV disease. Novel parameters have now been developed that have the potential to predict pathological aortic dilatation and may help to risk stratify BAV patients in future. This systematic review analyses the current 4D flow MRI literature after aortic valve and/or ascending aortic replacement in bicuspid aortic valve disease. 4D flow MRI has also identified distinct challenges posed by this cohort at the time of valve replacement compared to standard management of tri-leaflet disorders, and may help tailor the type and timing of replacement. Eccentric pathological flow patterns seen after bioprosthetic valve implantation, but not with mechanical prostheses, might be an important future consideration in intervention planning. 4D flow MRI also has promising potential in supporting the development of artificial valve prostheses and aortic conduits with more physiological flow patterns.

Keywords: bicuspid, bicuspid aortic valve, 4DFlow MRI, aortic, aortopathy, aortic valve replacement, transcatheter aortic valve implantation

INTRODUCTION

Bicuspid aortic valve (BAV) is the commonest congenital cardiac condition, affecting ∼0.5–1% of the general population (1). It is the leading cause of aortic valve disease under the age of 70 in developed countries and there is an increasingly recognized burden of disease associated. More than 20% of asymptomatic individuals will require surgical intervention in their young adult life (2) and at least 50% patients with BAV will undergo aortic valve replacement at some point in their lifetime (3). Aortopathy, another common comorbidity, occurs in association with BAV in 40–50% of adults (2). The risk of aortic dissection, often a catastrophic event, is ∼4%, far higher than the general population, therefore all BAV patients require surveillance (4). The thoracic aorta distal to the sinotubular junction is often not clearly visualized by echocardiography, therefore secondary imaging modalities are frequently required for detailed evaluation. Cardiovascular magnetic resonance imaging (MRI) is the preferred choice to cardiovascular computed tomography as repeated surveillance does not accumulate radiation exposure (5, 6).

Three-dimensional cine (time-resolved) phase contrast MRI with 3D velocity-encoding (4D flow MRI) offers a range of quantitative and qualitative tools to evaluate blood flow through the heart and great vessels over the cardiac cycle. 4D flow MRI has been validated for accuracy and consistency against two-dimensional phase contrast MRI (2D cine PC-MRI) (7) and the techniques have been optimized to now achieve image acquisition in less than 5 min (8). 4D flow MRI provides novel parameters that aid understanding of hemodynamic changes across the aortic valve and thoracic aorta that occur in BAV. 4D flow MRI has also contributed to the knowledge of flow disturbance after aortic valve replacement (AVR), and how this may differ in BAV.

Common 4D Flow MRI Parameters

In this review we will be concentrating on the 4D flow MRI parameters most frequently researched in BAV disease: helical flow, flow displacement/flow angle, and wall shear stress (WSS). The 4D flow MRI consensus statement presents a full summary of advanced imaging techniques available in vessel 4D flow MRI as well as their potential utility (8).

Helical Flow

Laminar flow describes the behavior of a viscous fluid along a pipe. This smooth flow is intrinsically related to the geometry of the vessel and the resistance to the flow (9). Early studies into 4D flow MRI observed the mild helical flow of blood as it travels along the arch of the aorta in normal subjects (10, 11). Helical rotation of blood consistently follows a right-handed (clockwise) pattern through the ascending aorta (AAo) and aortic arch, and this is preserved throughout life in health (10). Further to this, Kilner et al. discovered an individualized variation in this pattern that could be predicted by aortic arch curvature (11). Computational fluid dynamics (CFD), an alternative method of representing multidirectional flow volumes, has described the same right-handed helical nature of aortic arch blood flow and its crucial relationship to aortic geometry (12).

Initial studies of 4D flow MRI in BAV patients revealed markedly accentuated systolic flow patterns in the ascending aorta, with a more pronounced right-handed helix that persisted into the descending aorta, which is not seen in healthy subjects

(**Figure 1**) (13). 4D flow MRI used in conjunction with 2D analysis planes along the length of the thoracic aorta has allowed quantification of rotational flow (6). A 2013 study of 47 healthy volunteers was used to establish normal limits of helical flow to help differentiate between normal and increased right-handed helical flow providing classification of normal and abnormal aortic hemodynamics beyond subjective image interpretation (6). BAV patients with pathological right-handed helical flow had increased aortic diameters (indexed to body surface area) proportional to the severity of flow disturbance. Conversely, in a smaller group of BAV patients with normal flow patterns, the aortic size was similar to controls (6). This supports the hypothesis that helical flow is an important consideration in the pathogenesis of aortic dilatation in BAV. However, this method alone is not sufficient to determine the causal and temporal relationship of flow pattern and aortopathy.

Preliminary longitudinal studies of 4D flow MRI have examined the association between flow parameters and the rate of aortic growth. A small study of 19 children and young adults with BAV identified a positive correlation between baseline ascending aortic peak velocity and increased ascending aortic diameter growth (z-scores) at follow-up (14). However, deranged patient-specific helical flow patterns remained relatively stable during the study period (14).

Flow Displacement and Flow Angle

Another promising parameter for assessing aortic pathology is flow displacement. This is the difference between the central aortic valve plane and the point of maximum velocity-weighted forward flow (15). A similar parameter is the flow angle, the angle between the centerline and the systolic flow jet (16). Flow displacement is higher in BAV than in tricuspid aortic valves (TAV) for healthy and aortic-size matched controls (15). Mahadevia et al. reported a flow displacement, measured at the sinotubular junction (STJ), of 6–8 mm from the anatomical center (17). In a study of pediatric patients with BAV, den Raijer et al. reported that the angle of the systolic aortic flow jet was deviated by 17.5° from the anatomical axis of the aortic valve, compared to 10° in healthy volunteers (18). Furthermore, the flow jet angle was positively correlated with aortic diameters
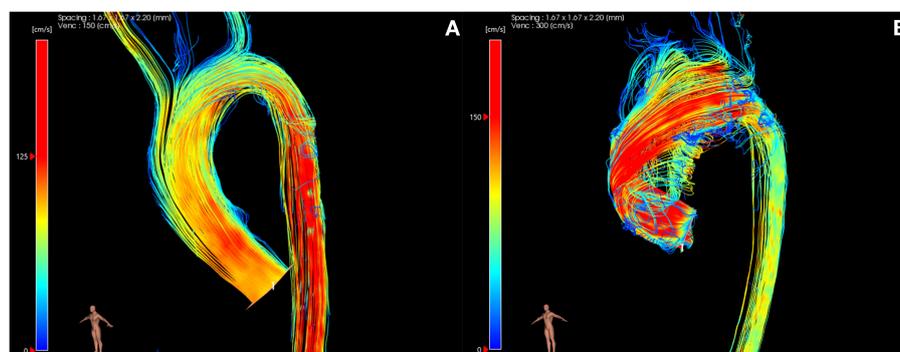

FIGURE 1 | 4D flow MRI images showing right-handed helical flow in normal **(A)** and BAV **(B)** subjects.

at the sinotubular junction and AAo, suggesting a association with aortic diameters in BAV patients. In addition, both flow jet angle and AAo diameter were significantly associated with elevated levels of matrix metallo-proteinase 2 (MMP-2), a protein implicated in vascular remodeling and aneurysm formation (18–20).

To date flow displacement has demonstrated the greatest predictive ability for aortic growth rate. In a small study of adults with BAV (average follow up 4.3 years), patients with higher flow displacement had a growth rate of 1.2 mm/year compared to 0.3 mm/year for other BAV patients (21). No patients had significant valvular impairment or other risk factors. Peak velocity was also correlated with growth rate (21). A similar study using 2D cine PC-MRI to measure baseline flow displacement found a strong correlation with clinically significant aortic growth over 3 years (22). The authors propose a threshold of 0.2, as above this level rates of growth were four times faster. Displacement was more predictive of aortic growth than baseline aortic diameter or any other flow parameter (22). This finding is supported by the relationship between restricted cusp opening angle, and therefore aortic flow deviation, with higher growth rate (23).

Wall Shear Stress

WSS is the frictional drag force exerted by flowing blood on the luminal surface of the vessel (24). It is a computed parameter that has been studied for its important role in the pathogenesis of a variety of conditions, including atherosclerosis and cerebral aneurysms (25–27). Multiple pathways have been identified, revealing endothelial cell morphology, alignment and gene expression alteration, as well as inflammation and dysregulation of the extracellular matrix in response to WSS stimuli (24–27). WSS quantification by 4D flow MRI uses analysis of spatial velocity gradients to calculate WSS as a vector quantity for complete arterial sections (28). Overall WSS can be split into axial (through-plane) and circumferential (in-plane) WSS.

BAV patients exhibit disturbed WSS in the AAo and aortic arch (6, 29, 30). In BAV patients with right-handed helical flow, peak systolic axial WSS is significantly raised compared to controls (6, 29). WSS is asymmetrical and eccentric in the AAo, with peak values on the right-anterior wall corresponding to flow jet direction (29). Circumferentially-averaged WSS ($WSS_{circavg}$) averages the WSS in a given 2D plane within the vessel and is persistently elevated in right-handed flow BAV patients, even at increasing aortic diameters (6, 30). This is in contrast to healthy volunteers, which demonstrate a decrease in $WSS_{circavg}$ as aortic diameter increases (6), resulting from the same blood volume traveling through a larger vessel and therefore exerting less friction against the vessel wall.

WSS distribution in the aorta in BAV has been modeled using CFD, and applied *in vitro* in a porcine aorta (31). On subsequent histological analysis, aortic tissue exposed to BAV WSS showed higher expression of MMP-2 and MMP-9 that was not seen in controls (31). McNally et al.'s *in vitro* experiments of non-dilated BAV aortas have demonstrated substantial flow and WSS disturbance that predicted the regions prone to dilatation (32). A landmark study by Guzzardi et al. confirmed these findings in humans and showed that the histopathological changes seen

in BAV aortopathy were only present in areas of high WSS, but not in those with normal or low WSS (33). These important findings indicate that WSS plays a vital role in initiating and driving aortic dilatation.

Aortic Dilation and Flow

To further clarify the impact of the aneurysmal aorta on flow, it is important to examine other causes of aortic dilatation. In a study of TAV patients with thoracic aortopathy (diameter >40 mm) from various etiologies, accentuated right-handed helical flow patterns were observed in nearly all patients (34). In patients with Marfan syndrome, normal flow patterns were seen in the AAo and arch, with local helix formation in the descending aorta (35). However, WSS was significantly lower than in healthy subjects with tricuspid valves (17). A further study by Bürk et al. found reduced WSS throughout the AAo and arch compared to age-matched controls, despite helical flow patterns being seen in aneurysm patients (36). This is in contrast to BAV, where WSS remains stable or increases as aortic size increases. Indeed, the areas of highest WSS correspond with the sites of aneurysm formation (32).

Aortic Surgery

Aortic diameter is linked to prognosis. Fifteen-year freedom from complications is 86% in patients with ascending aortic diameter less than 40 mm, but falls to 43% for diameter greater than 45 mm (37). Therefore, a key clinical priority is the identification and close monitoring of groups at risk of aortic growth. The presence of a bicuspid valve increases growth rate, with faster growth potentially linked to the aneurysm morphology (38). However, BAV patients still represent a heterogenous group of patients, some remaining asymptomatic into their old age, presenting a challenge for surgical (39).

The 25 year rate of aortic surgery in BAV is 25% (40). AVR is the commonest procedure and may be performed with or without aortic root replacement. Patients with BAV undergo AVR at a younger age than those with degenerative valve disease, and aortic stenosis is the most prevalent indication for valve intervention (41). The rate of proximal (Type A) aortic dissection post-AVR is reported to be 4–14%, though there is significant variation in the published literature (42, 43). Aortic rupture or re-dilatation requiring further surgery also occur (42). AVR has been associated with late aortic complications, but the mechanisms underlying this are not clear (41). There remains uncertainty amongst cardiac surgeons about whether prophylactic aortic replacement should be used to combat these risks in BAV patients (44). In this systematic review we conducted a comprehensive review of the 4D flow MRI literature in AVR and ascending aortic replacement.

METHODS

Eligibility Criteria

Studies which examined the use of 4D flow MRI for assessment of hemodynamic changes after Aortic Valve Replacement in Bicuspid Aortic Valve disease were included. Inclusion was limited to peer-reviewed literature, original reports, and human

FIGURE 2 | PRISMA flow diagram.
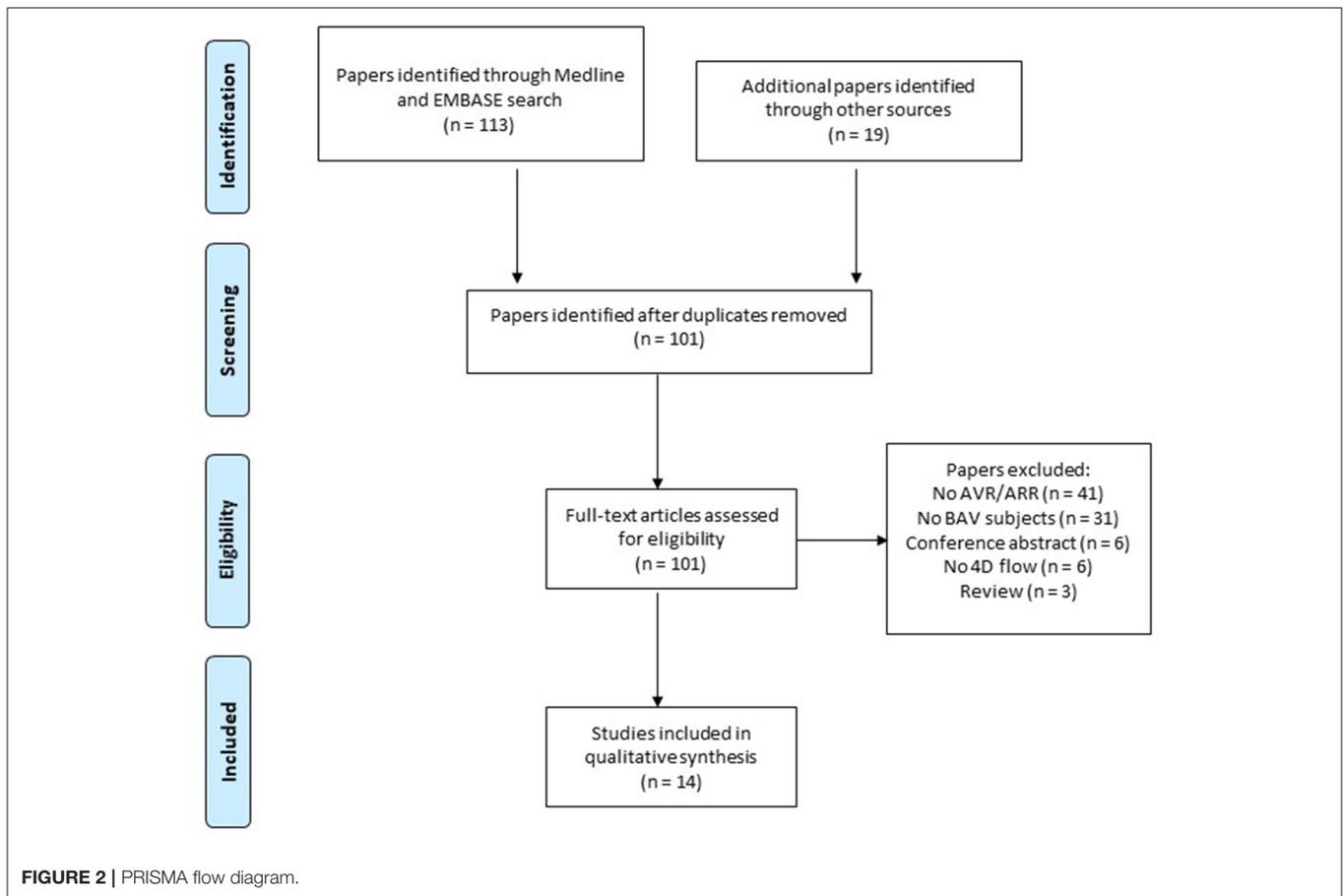
participants. Studies not published in English and solely *in vitro* experiments were excluded.

Search Strategy

A search of Medline and EMBASE was conducted for relevant literature. Search terms were identified, and searches were conducted using the PICO format: *bicuspid aortic valve*; *aortic valve replacement, aortic root replacement, aneurysm repair, ross procedure, TAVI*; *4D flow MRI, 4D flow CMR*. A search of additional sources included PubMed and reference lists of included studies. The search was carried out in February 2021.

Study Selection

Studies identified by the database search were assessed by two independent reviewers. The review of the proposed papers was conducted by DC (2 years experience as a doctor) and HP (4 years experience as a doctor). For disagreements, manuscripts were reviewed and decied upon by a third reviewer MB (11 years of 4D flow MRI research experience). PRISMA guidelines were used to identify relevant studies. Duplicate studies, review articles, conference abstracts, and those not meeting the search criteria were excluded. Papers using 4D flow MRI in Aortic Valve or Root Replacement were reviewed individually, and included if patients with bicuspid valves participated.

Results of the study selection are shown in the PRISMA flow diagram (**Figure 2**).

RESULTS

After a systematic search using multiple databases, we identified 101 studies for detailed consideration. After review of all full-text articles, a further 87 were excluded for the following reasons: did not mention aortic valve or root replacement (45); did not include BAV patients (31); did not use 4D flow MRI (6); conference abstracts (6); reviews (3). The remaining 14 studies were included for review of methodology and key results, with particular focus on Bicuspid Aortic Valve disease. The included papers are summarized in **Table 1** below.

The 14 selected papers studied a total of 447 participants (range 1–90). Five studies examined 4D flow MRI changes after isolated AVR, and of these two used bioprosthetic valves, two used pulmonary homografts (Ross procedure), and all five included mechanical valve types (46–50). The most commonly reported quantitative flow parameter was aortic WSS (4 out of 5 studies). No studies of TAVI were found that included BAV patients. Ten studies provided 4D flow data on ARR for patients with BAV aortopathy (47, 51–59). The majority

TABLE 1 | Summary table of included studies.

References	N	Study population	Surgical procedure		Valve type	4D flow Parameters				Main findings
			AVR	ARR		WSS	PV	FD/FA	Flow pattern	
Kamada et al. (46)	10	BAV & TAV Aortic stenosis	+		Mechanical				+	mAVR reduced Flow Angle and helicity density in the ascending aorta.
Bollache et al. (47)	53	BAV & TAV aortopathy	+	+	Mechanical, bioprosthetic, valve-sparing	+				Peak WSS reduced after mAVR but increased in ARR distal to the graft.
Bissell et al. (48)	90	BAV	+		Mechanical, bioprosthetic, Ross	+	+	+	+	Abnormal flow pattern in all after bAVR but only 27% after mAVR.
Farag et al. (49)	35	BAV	+		Mechanical (bileaflet)	+	+			Mean WSS after mAVR is greater than healthy control but similar to native BAV.
Von Knobelsdorff-Brenkenhoff et al. (50)	47	BAV & TAV	+		Mechanical, bioprosthetic, Ross	+			+	AVR resulted in asymmetrical flow and WSS compared to Ross and control.
Keller et al. (51)	20	BAV & TAV aortopathy	+	+	Mechanical				+	Reduction in abnormal flow patterns after mechanical ARR.
Collins et al. (52)	37	BAV & TAV aortopathy	+	+	Bioprosthetic, valve-sparing		+		+	Lower PV and improved flow pattern with valve-sparing ARR.
Condemi et al. (53)	1	BAV aortopathy		+	Valve-sparing	+			+	Reduced helicity but marked increase in velocity after ARR.
Stephens et al. (54)	24	BAV aortopathy		+	Valve-sparing	+			+	After ARR, Type 1 (R-L) had higher WSS compared to Type 0 BAV.
Allen et al. (55)	1	BAV aortopathy		+	Valve-sparing		+		+	Greatly increased PV after valve-sparing ARR.
Semaan et al. (56)	33	BAV & TAV aortopathy		+	Valve-sparing		+		+	Higher PV after ARR in bicuspid patients. Improved flow pattern after ARR in all.
Oechtering et al. (57)	36	BAV & TAV aortopathy		+	Valve-sparing				+	Altered flow patterns after ARR due to altered aortic geometry.
Gaudino et al. (58)	30	BAV & TAV aortopathy		+	Valve-sparing	+			+	Neosinus reconstruction resulted in physiologic vortices and reduced WSS.
Oechtering et al. (59)	30	BAV & TAV aortopathy		+	Valve-sparing		+		+	Similar sinus vortex pattern to healthy controls with valve-sparing sinus prosthesis.

AVR, aortic valve replacement; ARR, aortic root replacement; WSS, wall shear stress; PV, peak velocity; FD, flow displacement; FA, flow angle; BAV, bicuspid aortic valve; TAV, tricuspid aortic valve; mAVR, mechanical aortic valve replacement; bAVR, bioprosthetic aortic valve replacement.

(nine) of these studies used a valve-sparing technique (47, 52–59), with two using a mechanical prosthesis (47, 51) and two comparing valve-sparing and valved ARR (47, 52). All ARR studies reported data on the flow pattern or helicity in the aortic arch, with four also reporting WSS, and four reporting PV values. Three studies of isolated AVR identified by the initial search criteria did not provide characteristics of the native valve type of included patients (60–62). These were therefore not included in the summary table, however their results were deemed to be important in understanding post-operative hemodynamic changes, and have been reviewed below.

DISCUSSION

Isolated Aortic Valve Replacement

Aortic growth in BAV is accelerated compared to TAV pre-operatively. After AVR, aortic growth continues but is not different between these groups suggesting the AVR influences risk of late complications (63).

Flow characteristics undergo significant change after AVR. In one 4D flow study of patients with aortic stenosis before mechanical AVR and shortly afterwards, flow volume increased by 30% and flow angle in the ascending aorta reduced from 39° to 25°(46). The post-operative flow pattern in the AAo and arch showed a marked reduction in helicity, and streamlines appeared similar to normal volunteers. Furthermore, regional WSS reduced after AVR (47). In a study of 30 patients with BAV undergoing AVR, 73% of patients with mechanical AVR had normal flow patterns post-operatively, with reduced rotational WSS compared to unrepaired BAV controls (48). Flow angle also reduced, and flow displacement after mechanical AVR was similar to healthy subjects (**Figure 3**) (48). In patients receiving bileaflet mechanical AVR, mean and peak WSS were even lower than healthy volunteers (49). This suggests that these patients might be at lower risk of further aortic remodeling and subsequent dilation.

In contrast, patients who receive bioprosthetic AVR continue to exhibit highly abnormal flow patterns, with similar degrees
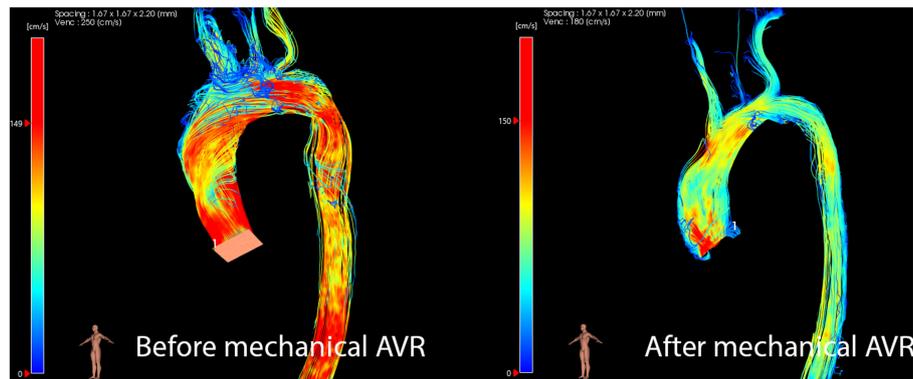
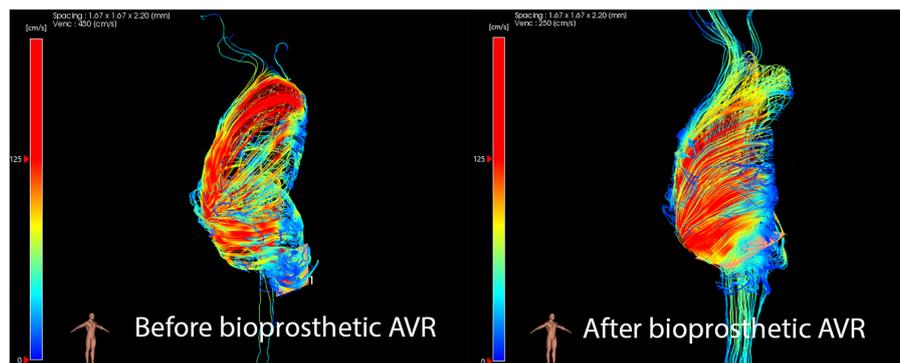**FIGURE 3 |** Flow profile normalizes after Mechanical AVR.

FIGURE 4 | Marked helical flow profile remains after bioprosthetic AVR.

of right-handed flow to unrepaired BAV controls (**Figure 4**) (48). When measured before and after surgery, rotational WSS and flow displacement did not change, and remained significantly higher than normal (48). In the same study, mechanical AVR patients had dramatically reduced WSS compared to pre-operative levels. However, in another study of 4 patients after bioprosthetic AVR, peak aortic WSS decreased in all patients compared to pre-operative imaging, but only to the level of unrepaired BAV controls. Both stented and stentless bioprostheses cause abnormal helicity and asymmetrical distribution of peak WSS, significantly higher than controls and mechanical AVR patients (50, 61). The flow eccentricity and helicity was slightly reduced in stentless valves, possibly due to the larger functional valve orifice and closer resemblance to normal TAV anatomy (50). Despite these drawbacks, bioprosthetic valves have many advantages including the avoidance of anticoagulation. Utilizing 4D flow MRI to design more physiological valve geometry may improve the longevity of bioprosthetic valves and minimize complications.

The Ross procedure offers a third option for patients needing AVR, involving autografting of the patient's native pulmonary valve to the aortic position. A new pulmonary valve is then usually reconstructed from cadaveric tissue (64). The procedure

is often conducted in childhood, as native tissue will grow with the child, and is often used in BAV patients. In the study by Bissell et al., ascending aortic rotational flow values after Ross procedure were similar to mechanical AVR and healthy subjects, and the majority had normal flow patterns (48). Systolic flow angles and flow displacement were also near-normal (48). Conaglen et al. reported that Ross patients had the lowest helicity of all valve types, and even had lower peak WSS than controls at the STJ (65). The Ross procedure therefore returns flow parameters to normal, likely explaining the favorable long-term outcomes with no significant ascending aortopathy, albeit often dilated sinuses (65). It is however technically complex to perform, and may require reintervention of both the right and left outflow tracts in later life (66).

Transcatheter aortic valve implantation (TAVI) is an alternative to AVR in patients with severe aortic stenosis, that avoids the need for sternotomy and cardiopulmonary bypass. To date few studies have examined the hemodynamic effects after TAVI, and none have included BAV patients. One report found TAVI results in increased flow eccentricity and flow displacement in the AAo compared to surgical AVR and controls (62). Others have shown reduced helical flow with TAVI (Edwards Sapien XT) compared to bioprosthetic AVR, but still abnormal compared

Aortic Root Replacement

Prophylactic aortic root replacement is often considered at the time of AVR in patients with aortopathy to mitigate the risk of future aortic dissection. The Modified Bentall procedure is the standard technique, consisting of a synthetic ascending aorta and root graft with a bioprosthetic or mechanical valve (68). A large study has demonstrated the low rate of long-term aortic complications with this technique (69). Previous guidelines established aortic size thresholds for surgical intervention, however these are predominantly based on connective tissue disorders such as Marfan syndrome (70). Clinical data suggest aortic growth and late complication rates differ in BAV compared to intrinsic aortopathies (71). Additionally, so far there is no evidence for accelerated aortic growth rate after AVR compared to prophylactic aortic root replacement (72).

Using 4D flow MRI, hemodynamic effects of the synthetic aortic root graft can be examined in more detail. On blinded visual assessment of helical flow patterns, pre and postoperatively, aortic root replacement with a mechanical (On-X) valve returns flow distortion to normal (51). Peak transvalvular pressure gradients are similar when measured with 4D flow MRI and Doppler echocardiography, and show a decrease after mechanical ARR (51). However, helical flow remains highly abnormal after ARR with a bioprosthetic valve (52). Peak velocities also remain elevated compared to controls and persist into the aortic arch and descending aorta (52). Abnormally high WSS develops in the aorta immediately distal to the graft when assessed before and after ARR with hemi-arch replacement in one study (47); this raises concerns for further remodeling in this region. A possible explanation for this is the reduced compliance of the aortic graft material resulting in increased flow velocities (73). The stiffer material results in loss of the Windkessel effect of large elastic arteries, whereby hydraulic energy is stored in distensible vessels during systole and discharged during diastole, therefore energy loss occurs after ARR (73, 74). This poses the question whether prophylactic ARR just defers the ongoing hemodynamically driven aortic dilation further downstream.

Valve-Sparing Aortic Root Replacement

For patients with aortopathy and adequate valve function, valve-sparing aortic root replacement is another surgical option for the prevention of aortic complications. This technique is gaining popularity, particularly in younger patients where retaining the native valve is desirable. However, the procedure, developed for tricuspid aortopathies, requires consideration of individual valve geometry if used in BAV. Several reports have examined the flow characteristics after valve-sparing thoracic aortic aneurysm repair in BAV patients (53–55). Similar to valved conduits, valve-sparing aortic root replacement results in higher flow velocities throughout the thoracic aorta (52, 56). Flow velocity increases after surgical repair resulting in higher WSS in the graft and
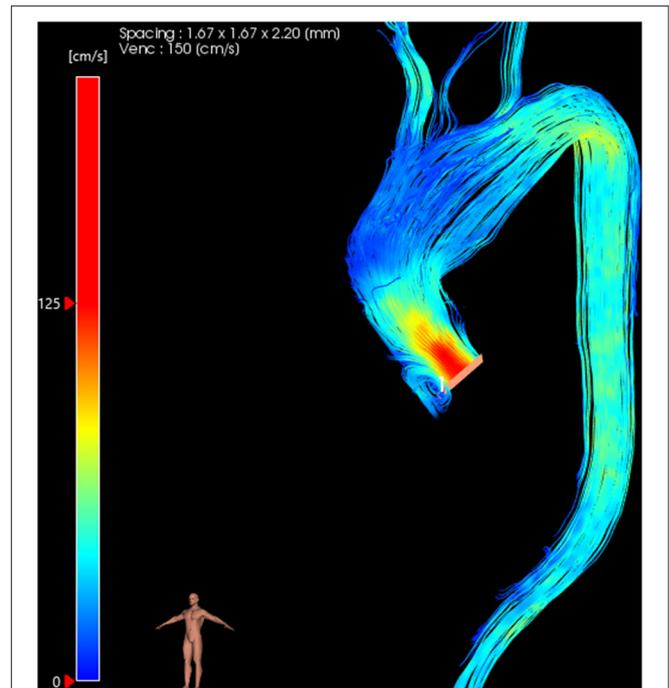

FIGURE 5 | Vortical flow after aortic root replacement.

distal aortic regions (55). Two studies have directly compared valve-sparing and valved aortic root replacement, and have demonstrated significantly higher peak velocity and WSS with the valve-sparing technique, particularly in regions distal to the graft (47, 52).

Flow velocity is significantly higher and more eccentric when the reimplanted native valve is bicuspid compared to tricuspid (56). Flow distortion may be exaggerated further by BAV cusp morphology. Stephens et al. evaluated 19 BAV patients after valve-sparing aortic root replacement and found that left-right coronary cusp fusion BAV had elevated and asymmetric WSS throughout the AAo (54). In contrast "purely bicuspid" BAV patients with a single midline commissure had significantly lower WSS similar to healthy TAV controls (54). This may influence long-term risk of distal complications, although longitudinal studies are needed.

Aortic reconstruction may also disturb normal aortic root physiology, as assessed by 4D flow MRI. Systolic flow vortices in the Sinus of Valsalva (SOV) occur after peak systole and persist until diastole and are thought to have an important role in valve closure and coronary perfusion (**Figure 5**) (75). Valve-sparing aortic root replacement, by either the David or Yacoub technique, involves excision of the native Sinus of Valsalva (68). This loss of sinus architecture abolishes vortical flow and may have longer term consequences. New techniques to reconstruct neosinuses during valve-sparing aortic root replacement are effective at restoring vortical supravalvular flow and reducing WSS in the ascending aorta (58, 59, 76).

All valve-sparing aortic root replacement recipients display altered aortic geometry compared to the round shape of healthy

controls. This is most often due to kinking of the graft or the distal anastomosis and is observed in around 90% of valve-sparing aortic root replacement patients. Altered geometry is associated with the development of deviated flow patterns (57, 59). In the only longitudinal study of 4D flow MRI after valve-sparing aortic root replacement, 12 patients with Marfan syndrome were followed for an average of 8 years post-operatively (77). One patient developed a Stanford Type B aortic dissection, after demonstrating highly abnormal helical flow patterns and higher normalized flow displacement compared to the other patients (4.5 vs. 1.8%). WSS on the right anterior wall of the ascending aorta was also higher than others in this case (78). Another report found an association with abnormal flow and aneurysm formation after surgery for aortic coarctation (77). To date no longitudinal 4D flow MRI data on BAV patents after valve-sparing aortic root replacement.

Limitations of 4D Flow MRI

The acquisition of 4D flow MRI data requires additional sequences to be added during the MRI scan which are not always readily available to the clinician. There is the potential for variation in data depending on the equipment (1.5 vs. 3.0T MRI) and sequence used. Further variation can be introduced with the use of different post-processing platforms. Gadolinium-based contrast may sometimes be required during clinical protocols, however this is unlikely to negatively influence 4D flow acquisition and may even enhance flow visualization (79).

While 4D flow MRI has been validated in numerous studies, it is important for individual sequence set up to undergo validation against the local gold standards. Doppler echocardiography is clinically established for measurement of peak velocity and is considered a surrogate gold standard. It is important to also acknowledge that the typically low temporal resolution of 4D flow MRI (40–50 ms) could fail to capture the peak jet, and therefore some underestimation is likely. 2D cine PC-MRI is the gold standard for total forward flow comparison, which is less affected by lower temporal resolution.

CONCLUSION

BAV disease presents specific management considerations at the time of surgery and thereafter. 4D flow MRI presents a promising clinical tool to identify BAV patients who may be at risk of developing a more severe aortopathy phenotype, with progressive aneurysm formation and risk of dissection. However, further large prospective studies are needed to confirm this prognostic value for patients and clinicians. 4D flow MRI also shows promising value in supporting the development of artificial valve prostheses and aortic conduits with more physiological flow patterns. The inferior performance of bioprosthetic valves compared to mechanical prostheses in 4D flow studies may explain late post-operative complications and offers opportunities for improved valve design. Valve morphology and the consequent flow patterns are crucial when considering valve-sparing aortic root replacement, and further longitudinal data is needed on the outcomes for patients with bicuspid valves. 4D flow MRI is now fast enough to allow wide spread clinical integration leading to easier facilitation of large multi-center trials.

REFERENCES

1. Basso C, Boschello M, Perrone C, Mecenero A, Cera A, Bicego D, et al. An echocardiographic survey of primary school children for bicuspid aortic valve. *Am J Cardiol.* (2004) 93:661–3. doi: 10.1016/j.amjcard.2003.11.031

2. Tzemos N, Therrien J, Yip J, Thanassoulis G, Tremblay S, Jamorski MT, et al. Outcomes in adults with bicuspid aortic valves. *JAMA J Am Med Assoc.* (2008) 300:1317–25. doi: 10.1001/jama.300.11.1317

3. Michelena HI, Prakash SK, Corte A Della, Bissell MM, Anavekar N, Mathieu P, et al. Bicuspid aortic valve identifying knowledge gaps and rising to the challenge from the international bicuspid aortic valve consortium (BAVCON). *Circulation.* (2014) 129:2691–704. doi: 10.1161/CIRCULATIONAHA.113.007851

4. Siu SC, Silversides CK. Bicuspid Aortic Valve Disease. *J Am Coll Cardiol.* (2010) 55:2789–800. doi: 10.1016/j.jacc.2009.12.068

5. Baumgartner H, De Backer J, Babu-Narayan SV, Budts W, Chessa M, Diller G-P, et al. 2020 ESC Guidelines for the management of adult congenital heart disease. *Eur Heart J.* (2020) 42:563–645. doi: 10.1093/eurheartj/ehaa554

6. Bissell MM, Hess AT, Biasiolli L, Glaze SJ, Loudon M, Pitcher A, et al. Aortic dilation in bicuspid aortic valve disease: flow pattern is a major contributor and differs with valve fusion type. *Circ Cardiovasc Imaging.* (2013) 6:499–507. doi: 10.1161/CIRCIMAGING.113.000528

7. Warmerdam E, Krings GJ, Leiner T, Grotenhuis HB. Three-dimensional and four-dimensional flow assessment in congenital heart disease. *Heart.* (2019) 106:421–6. doi: 10.1136/heartjnl-2019-315797

8. Dyverfeldt P, Bissell M, Barker AJ, Bolger AF, Carlhäll CJ, Ebbers T, et al. 4D flow cardiovascular magnetic resonance consensus statement. *J Cardiovasc Magn Reson.* (2015) 17:72. doi: 10.1186/s12968-015-0174-5

9. Pfitzner J. Poiseuille and his law. *Anaesthesia.* (1976) 31:273–5. doi: 10.1111/j.1365-2044.1976.tb11804.x

10. Bogren HG, Buonocore MH. 4D magnetic resonance velocity mapping of blood flow patterns in the aorta in young vs. elderly normal subjects. *J Magn Reson Imaging.* (1999) 10:861–9. doi: 10.1002/(SICI)1522-2586(199911)10:5<861::AID-JMRI35>3.0.CO;2-E

11. Kilner PJ, Yang GZ, Mohiaddin RH, Firmin DN, Longmore DB. Helical and retrograde secondary flow patterns in the aortic arch studied by

three-directional magnetic resonance velocity mapping. *Circulation.* (1993) 88:2235–47. doi: 10.1161/01.CIR.88.5.2235

12. Tse KM, Chang R, Lee HP, Lim SP, Venkatesh SK, Ho P. A computational fluid dynamics study on geometrical influence of the aorta on haemodynamics. *Eur J Cardiothorac Surg.* (2013) 43:829–38. doi: 10.1093/ejcts/ezs388

13. Hope MD, Hope TA, Meadows AK, Ordovas KG, Urbania TH, Alley MT, et al. Bicuspid aortic valve: Four-dimensional MR evaluation of ascending aortic systolic flow patterns. *Radiology.* (2010) 255:53–61. doi: 10.1148/radiol.09091437

14. Rose MJ, Rigsby CK, Berhane H, Bollache E, Jarvis K, Barker AJ, et al. 4-D flow MRI aortic 3-D hemodynamics and wall shear stress remain stable over short-term follow-up in pediatric and young adult patients with bicuspid aortic valve. *Pediatr Radiol.* (2019) 49:57–67. doi: 10.1007/s00247-018-4257-y

15. Garcia J, Barker AJ, Murphy I, Jarvis K, Schnell S, Collins JD, et al. Four-dimensional flow magnetic resonance imaging-based characterization of aortic morphometry and haemodynamics: impact of age, aortic diameter, and valve morphology. *Eur Heart J Cardiovasc Imaging.* (2016) 17:877–84. doi: 10.1093/ehjci/jev228

16. Sigovan M, Hope MD, Dyverfeldt P, Saloner D. Comparison of four-dimensional flow parameters for quantification of flow eccentricity in the ascending aorta. *J Magn Reson Imaging.* (2011) 34:1226–30. doi: 10.1002/jmri.22800

17. Mahadevia R, Barker AJ, Schnell S, Entezari P, Kansal P, Fedak PWM, et al. Bicuspid aortic cusp fusion morphology alters aortic three-dimensional outflow patterns, wall shear stress, and expression of aortopathy. *Circulation.* (2014) 129:673–82. doi: 10.1161/CIRCULATIONAHA.113.003026

18. Den Reijer PM, Sallee D, Van Der Velden P, Zaaijer E, Parks WJ, Ramamurthy S, et al. Hemodynamic predictors of aortic dilatation in bicuspid aortic valve by velocity-encoded cardiovascular magnetic resonance. *J Cardiovasc Magn Reson.* (2010) 12:4. doi: 10.1186/1532-429X-12-4

19. Galis ZS, Khatri JJ. Matrix metalloproteinases in vascular remodeling and atherogenesis: the good, the bad, and the ugly. *Circ Res.* (2002) 90:251–62. doi: 10.1161/res.90.3.251

20. Sangiorgi G, Trimarchi S, Mauriello A, Righini P, Bossone E, Suzuki T, et al. Plasma levels of metalloproteinases-9 and−2 in the acute and subacute phases of type A and type B aortic dissection. *J Cardiovasc Med.* (2006) 7:307–15. doi: 10.2459/01.JCM.0000223251.26988.c5

21. Hope MD, Sigovan M, Wrenn SJ, Saloner D, Dyverfeldt P. MRI hemodynamic markers of progressive bicuspid aortic valve-related aortic disease. *J Magn Reson Imaging.* (2014) 40:140–5. doi: 10.1002/jmri.24362

22. Burris NS, Sigovan M, Knauer HA, Tseng EE, Saloner D, Hope MD. Systolic flow displacement correlates with future ascending aortic growth in patients with bicuspid aortic valves undergoing magnetic resonance surveillance. *Invest Radiol.* (2014) 49:635–9. doi: 10.1097/RLI.0000000000000064

23. Della Corte A, Bancone C, Conti CA, Votta E, Redaelli A, Del Viscovo L, et al. Restricted cusp motion in right-left type of bicuspid aortic valves: a new risk marker for aortopathy. *J Thorac Cardiovasc Surg.* (2012) 144:360–9.e1. doi: 10.1016/j.jtcvs.2011.10.014

24. Dolan JM, Meng H, Singh S, Paluch R, Kolega J. High fluid shear stress and spatial shear stress gradients affect endothelial proliferation, survival, and alignment. *Ann Biomed Eng.* (2011) 39:1620–31. doi: 10.1007/s10439-011-0267-8

25. DePaola N, Gimbrone MA, Davies PF, Dewey CF. Vascular endothelium responds to fluid shear stress gradients. *Arterioscler Thromb.* (1992) 12:1254–7. doi: 10.1161/01.atv.12.11.1254

26. Gimbrone MA. Endothelial dysfunction, hemodynamic forces, and atherosclerosis. *Thromb Haemost.* 82:722–26. doi: 10.1055/s-0037-1615903

27. Meng H, Wang Z, Hoi Y, Gao L, Metaxa E, Swartz DD, et al. Complex hemodynamics at the apex of an arterial bifurcation induces vascular remodeling resembling cerebral aneurysm initiation. *Stroke.* (2007) 38:1924–31. doi: 10.1161/STROKEAHA.106.481234

28. Stalder AF, Russe MF, Frydrychowicz A, Bock J, Hennig J, Markl M. Quantitative 2D and 3D phase contrast MRI: optimized analysis of blood flow and vessel wall parameters. *Magn Reson Med.* (2008) 60:1218–31. doi: 10.1002/mrm.21778

29. Barker AJ, Markl M, Bürk J, Lorenz R, Bock J, Bauer S, et al. Bicuspid aortic valve is associated with altered wall shear stress

30. Rodríguez-Palomares JF, Dux-Santoy L, Guala A, Kale R, Maldonado G, Teixidó-Turà G, et al. Aortic flow patterns and wall shear stress maps by 4D-flow cardiovascular magnetic resonance in the assessment of aortic dilatation in bicuspid aortic valve disease. *J Cardiovasc Magn Reson.* (2018) 20:28. doi: 10.1186/s12968-018-0451-1

31. Atkins SK, Cao K, Rajamannan NM, Sucosky P. Bicuspid aortic valve hemodynamics induces abnormal medial remodeling in the convexity of porcine ascending aortas. *Biomech Model Mechanobiol.* (2014) 13:1209–25. doi: 10.1007/s10237-014-0567-7

32. McNally A, Madan A, Sucosky P. Morphotype-dependent flow characteristics in bicuspid aortic valve ascending aortas: a benchtop particle image velocimetry study. *Front Physiol.* (2017) 8:44. doi: 10.3389/fphys.2017.00044

33. Guzzardi DG, Barker AJ, Van Ooij P, Malaisrie SC, Puthumana JJ, Belke DD, et al. Valve-related hemodynamics mediate human bicuspid aortopathy: insights from wall shear stress mapping. *J Am Coll Cardiol.* (2015) 66:892–900. doi: 10.1016/j.jacc.2015.06.1310

34. Hope TA, Markl M, Wigström L, Alley MT, Miller DC, Herfkens RJ. Comparison of flow patterns in ascending aortic aneurysms and volunteers using four-dimensional magnetic resonance velocity mapping. *J Magn Reson Imaging.* (2007) 26:1471–9. doi: 10.1002/jmri.21082

35. Geiger J, Markl M, Herzer L, Hirtler D, Loeffelbein F, Stiller B, et al. Aortic flow patterns in patients with Marfan syndrome assessed by flow-sensitive four-dimensional MRI. *J Magn Reson Imaging.* (2012) 35:594–600. doi: 10.1002/jmri.23500

36. Bürk J, Blanke P, Stankovic Z, Barker A, Russe M, Geiger J, et al. Evaluation of 3D blood flow patterns and wall shear stress in the normal and dilated thoracic aorta using flow-sensitive 4D CMR. *J Cardiovasc Magn Reson.* (2012) 14:84. doi: 10.1186/1532-429X-14-84

37. Borger MA, Preston M, Ivanov J, Fedak PWM, Davierwala P, Armstrong S, et al. Should the ascending aorta be replaced more frequently in patients with bicuspid aortic valve disease? *J Thorac Cardiovasc Surg.* (2004) 128:677–83. doi: 10.1016/j.jtcvs.2004.07.009

38. Della Corte A, Bancone C, Dialetto G, Covino FE, Manduca S, Montibello M V, et al. The ascending aorta with bicuspid aortic valve: a phenotypic classification with potential prognostic significance. *Eur J Cardiothorac Surg.* (2014) 46:240–7; discussion 247. doi: 10.1093/ejcts/ezt621

39. Mordi I, Tzemos N. Bicuspid aortic valve disease: a comprehensive review. *Cardiol Res Pract.* (1960) 2012: 196037. doi: 10.1155/2012/196037

40. Michelena HI, Khanna AD, Mahoney D, Margaryan E, Topilsky Y, Suri RM, et al. Incidence of aortic complications in patients with bicuspid aortic valves. *JAMA J Am Med Assoc.* (2011) 306:1104–12. doi: 10.1001/jama.2011.1286

41. Girdauskas E, Disha K, Borger MA, Kuntze T. Risk of proximal aortic dissection in patients with bicuspid aortic valve: how to address this controversy? *Interact Cardiovasc Thorac Surg.* (2013) 18:355–9. doi: 10.1093/icvts/ivt518

42. Matsuyama K, Usui A, Akita T, Yoshikawa M, Murayama M, Yano T, et al. Natural history of a dilated ascending aorta after aortic valve replacement. *Circ J.* (2005) 69:392–6. doi: 10.1253/circj.69.392

43. Tsutsumi K, Inoue Y, Hashizume K, Kimura N, Takahashi R. Risk factor analysis for acute type A aortic dissection after aortic valve replacement. *Gen Thorac Cardiovasc Surg.* (2010) 58:601–5. doi: 10.1007/s11748-010-0658-z

44. Verma S, Yanagawa B, Kalra S, Ruel M, Peterson MD, Yamashita MH, et al. Knowledge, attitudes, and practice patterns in surgical management of bicuspid aortopathy: a survey of 100 cardiac surgeons. *J Thorac Cardiovasc Surg.* (2013) 146:1033–40.e4. doi: 10.1016/j.jtcvs.2013.06.037

45. Davies RR, Kaple RK, Mandapati D, Gallo A, Botta DM, Elefteriades JA, et al. Natural history of ascending aortic aneurysms in the setting of an unreplaced bicuspid aortic valve. *Ann Thorac Surg.* (2007) 83:1338–44. doi: 10.1016/j.athoracsur.2006.10.074

46. Kamada H, Ota H, Nakamura M, Imai Y, Ishida S, Sun W, et al. Perioperative hemodynamic changes in the thoracic aorta in patients with aortic valve stenosis: a prospective serial 4D-Flow MRI Study. *Semin Thorac Cardiovasc Surg.* (2019) 32:25–34. doi: 10.1053/j.semtcvs.2019.07.006

47. Bollache E, Fedak PWM, van Ooij P, Rahman O, Malaisrie SC, McCarthy PM, et al. Perioperative evaluation of regional aortic wall shear stress patterns in patients undergoing aortic valve and/or proximal thoracic

aortic replacement. *J Thorac Cardiovasc Surg.* (2018) 155:2277–86.e2. doi: 10.1016/j.jtcvs.2017.11.007

48. Bissell MM, Loudon M, Hess AT, Stoll V, Orchard E, Neubauer S, et al. Differential flow improvements after valve replacements in bicuspid aortic valve disease: A cardiovascular magnetic resonance assessment. *J Cardiovasc Magn Reson.* (2018) 20:10. doi: 10.1186/s12968-018-0431-5

49. Farag ES, Schade EL, van Ooij P, Boekholdt SM, Planken RN, van Kimmenade R, et al. Bileaflet mechanical aortic valves do not alter ascending aortic wall shear stress. *Int J Cardiovasc Imaging.* (2019) 35:703–10. doi: 10.1007/s10554-018-1508-9

50. Von Knobelsdorff-Brenkenhoff F, Trauzeddel RF, Barker AJ, Gruettner H, Markl M, Schulz-Menger J. Blood flow characteristics in the ascending aorta after aortic valve replacement - A pilot study using 4D-flow MRI. *Int J Cardiol.* (2014) 170:426–33. doi: 10.1016/j.ijcard.2013.11.034

51. Keller EJ, Malaisrie SC, Kruse J, McCarthy PM, Carr JC, Markl M, et al. Reduction of aberrant aortic haemodynamics following aortic root replacement with a mechanical valved conduit. *Interact Cardiovasc Thorac Surg.* (2016) 23:416–23. doi: 10.1093/icvts/ivw173

52. Collins JD, Semaan E, Barker A, McCarthy PM, Carr JC, Markl M, et al. Comparison of hemodynamics after aortic root replacement using valve-sparing or bioprosthetic valved conduit. *Ann Thorac Surg.* (2015) 100:1556–62. doi: 10.1016/j.athoracsur.2015.04.109

53. Condemi F, Campisi S, Viallon M, Croisille P, Fuzelier JF, Avril S. Ascending thoracic aorta aneurysm repair induces positive hemodynamic outcomes in a patient with unchanged bicuspid aortic valve. *J Biomech.* (2018) 81:145–8. doi: 10.1016/j.jbiomech.2018.09.022

54. Stephens EH, Hope TA, Kari FA, Kvitting JPE, Liang DH, Herfkens RJ, et al. Greater asymmetric wall shear stress in Sievers' type 1/LR compared with 0/LAT bicuspid aortic valves after valve-sparing aortic root replacement. *J Thorac Cardiovasc Surg.* (2015) 150:59–68. doi: 10.1016/j.jtcvs.2015.04.020

55. Allen BD, Barker AJ, Kansal P, Collins JD, Carr JC, Malaisrie SC, et al. Impact of aneurysm repair on thoracic aorta hemodynamics. *Circulation.* (2013) 128:e341–3. doi: 10.1161/CIRCULATIONAHA.112.000850

56. Semaan E, Markl M, Malaisrie SC, Barker A, Allen B, Mccarthy P, et al. Haemodynamic outcome at four-dimensional flow magnetic resonance imaging following valve-sparing aortic root replacement with tricuspid and bicuspid valve morphology. *Eur J Cardiothorac Surg.* (2013) 45:818–25. doi: 10.1093/ejcts/ezt526

57. Oechtering TH, Sieren MM, Hunold P, Hennemuth A, Huellebrand M, Scharfschwerdt M, et al. Time-resolved 3-dimensional magnetic resonance phase contrast imaging (4D Flow MRI) reveals altered blood flow patterns in the ascending aorta of patients with valve-sparing aortic root replacement. *J Thorac Cardiovasc Surg.* (2020) 159:798–810.e1. doi: 10.1016/j.jtcvs.2019.02.127

58. Gaudino M, Piatti F, Lau C, Sturla F, Weinsaft JW, Weltert L, et al. Aortic flow after valve sparing root replacement with or without neosinuses reconstruction. *J Thorac Cardiovasc Surg.* (2019) 157:455–65. doi: 10.1016/j.jtcvs.2018.06.094

59. Oechtering TH, Hons CF, Sieren M, Hunold P, Hennemuth A, Huellebrand M, et al. Time-resolved 3-dimensional magnetic resonance phase contrast imaging (4D Flow MRI) analysis of hemodynamics in valve-sparing aortic root repair with an anatomically shaped sinus prosthesis. *J Thorac Cardiovasc Surg.* (2016) 152:418–27.e1. doi: 10.1016/j.jtcvs.2016.04.029

60. Trauzeddel RF, Löbe U, Barker AJ, Gelsinger C, Butter C, Markl M, et al. Blood flow characteristics in the ascending aorta after TAVI compared to surgical aortic valve replacement. *Int J Cardiovasc Imaging.* (2016) 32:461–7. doi: 10.1007/s10554-015-0792-x

61. van Kesteren F, Wollersheim LW, Baan J, Nederveen AJ, Kaya A, Boekholdt SM, et al. Four-dimensional flow MRI of stented versus stentless aortic valve bioprostheses. *Eur Radiol.* (2018) 28:257–64. doi: 10.1007/s00330-017-4953-2

62. Farag ES, Vendrik J, van Ooij P, Poortvliet QL, van Kesteren F, Wollersheim LW, et al. Transcatheter aortic valve replacement alters ascending aortic blood flow and wall shear stress patterns: a 4D flow MRI

comparison with age-matched, elderly controls. *Eur Radiol.* (2019) 29:1444–51. doi: 10.1007/s00330-018-5672-z

63. Regeer M V., Versteegh MIM, Klautz RJM, Schalij MJ, Bax JJ, Marsan NA, et al. Effect of aortic valve replacement on aortic root dilatation rate in patients with bicuspid and tricuspid aortic valves. *Ann Thorac Surg.* (2016) 102:1981–7. doi: 10.1016/j.athoracsur.2016.05.038

64. Um KJ, Mcclure GR, Belley-Cote EP, Gupta S, Bouhout I, Lortie H, et al. Hemodynamic outcomes of the Ross procedure versus other aortic valve replacement: a systematic review and meta-analysis. *J Cardiovasc Surg.* (2018) 59:462–70. doi: 10.23736/S0021-9509.18.10255-2

65. Conaglen P, Luthra S, Skillington P. Comparison of reduction ascending aortoplasty and ascending aortic replacement for bicuspid valve related aortopathy in young adult patients undergoing aortic valve replacement-long-term follow-up. *Hear Lung Circ.* (2009) 18:337–42. doi: 10.1016/j.hlc.2009.03.049

66. Etnel JRG, Elmont LC, Ertekin E, Mokhles MM, Heuvelman HJ, Roos-Hesselink JW, et al. Outcome after aortic valve replacement in children: a systematic review and meta-analysis. *J Thorac Cardiovasc Surg.* (2016) 151:143–52.e3. doi: 10.1016/j.jtcvs.2015.09.083

67. Kanjanahattakij N, Horn B, Vutthikraivit W, Biso SM, Ziccardi MR, Lu MLR, et al. Comparing outcomes after transcatheter aortic valve replacement in patients with stenotic bicuspid and tricuspid aortic valve: a systematic review and meta-analysis. *Clin Cardiol.* (2018) 41:896–902. doi: 10.1002/clc.22992

68. Groner LK, Lau C, Devereux RB, Green DB. Imaging of the Postsurgical Aorta in Marfan Syndrome. *Curr Treat Options Cardiovasc Med.* (2018) 20:1–25. doi: 10.1007/s11936-018-0675-2

69. Gott VL, Greene PS, Alejo DE, Cameron DE, Naftel DC, Miller DC, et al. Replacement of the Aortic Root in Patients with Marfan's Syndrome. *N Engl J Med.* (1999) 340:1307–13. doi: 10.1056/NEJM199904293401702

70. Hiratzka LF, Bakris GL, Beckman JA, Bersin RM, Carr VF, Casey DE, et al. 2010 ACCF/AHA/AATS/ACR/ASA/SCA/SCAI/SIR/STS/SVM Guidelines for the diagnosis and management of patients with thoracic aortic disease. *J Am Coll Cardiol.* (2010) 55:e27–129. doi: 10.1016/j.jacc.2010.02.015

71. Itagaki S, Chikwe JP, Chiang YP, Egorova NN, Adams DH. Long-term risk for aortic complications after aortic valve replacement in patients with bicuspid aortic valve versus marfan syndrome. *J Am Coll Cardiol.* (2015) 65:2363–9. doi: 10.1016/j.jacc.2015.03.575

72. Lee SH, Kim JB, Kim DH, Jung SH, Choo SJ, Chung CH, et al. Management of dilated ascending aorta during aortic valve replacement: valve replacement alone versus aorta wrapping versus aorta replacement. *J Thorac Cardiovasc Surg.* (2013) 146:802–9. doi: 10.1016/j.jtcvs.2013.06.007

73. Kim SY, Hinkamp TJ, Jacobs WR, Lichtenberg RC, Posniak H, Pifarré R. Effect of an inelastic aortic synthetic vascular graft on exercise hemodynamics. *Ann Thorac Surg.* (1995) 59:981–9. doi: 10.1016/0003-4975(95)00068-V

74. Morita S, Asou T, Kuboyama I, Harasawa Y, Sunagawa K, Yasui H. Inelastic vascular prosthesis for proximal aorta increases pulsatile arterial load and causes left ventricular hypertrophy in dogs. *J Thorac Cardiovasc Surg.* (2002) 124:768–74. doi: 10.1067/mtc.2002.124244

75. Escobar Kvitting JP, Ebbers T, Wigström L, Engvall J, Olin CL, Bolger AF. Flow patterns in the aortic root and the aorta studied with time-resolved, 3-dimensional, phase-contrast magnetic resonance imaging: implications for aortic valve-sparing surgery. *J Thorac Cardiovasc Surg.* (2004) 127:1602–7. doi: 10.1016/j.jtcvs.2003.10.042

76. Galea N, Piatti F, Sturla F, Weinsaft JW, Lau C, Chirichilli I, et al. Novel insights by 4D Flow imaging on aortic flow physiology after valve-sparing root replacement with or without neosinuses. *Interact Cardiovasc Thorac Surg.* (2018) 26:957–64. doi: 10.1093/icvts/ivx431

77. Crook SES, Hope MD. Arch hypoplasia and aneurysm after aortic coarctation repair: abnormal flow may be the link. *JACC Cardiovasc Imaging.* (2011) 4:685–6. doi: 10.1016/j.jcmg.2011.02.016

78. Hope TA, Kvitting JPE, Hope MD, Miller DC, Markl M, Herfkens RJ. Evaluation of Marfan patients status post valve-sparing aortic root replacement with 4D flow. *Magn Reson Imaging.* (2013) 31:1479–84. doi: 10.1016/j.mri.2013.04.003

79. Bock J, Frydrychowicz A, Stalder AF, Bley TA, Burkhardt H, Hennig J, et al. 4D phase contrast MRI at 3 T: Effect of standard and

blood-pool contrast agents on SNR, PC-MRA, and blood flow visualization. *Magn Reson Med.* (2010) 63:330–8. doi: 10.1002/mrm. 22199

Conflict of Interest: The authors declare that the research was conducted in the absence of any commercial or financial relationships that could be construed as a potential conflict of interest.